PHASE DELAY AND ENERGY FLOW IN ANGULARLY DISPERSIVE OPTICAL SYSTEMS

by

Michael Ware

March 1, 1999

Submitted to Brigham Young University in partial fulfillment
of graduation requirements for University Honors

Advisor: Justin Peatross

Signature:_____

Honors Dean: Steven Benzley

Signature:_____

ABSTRACT

Angularly dispersive systems introduce frequency dependent phase shifts to the frequency components of laser pulses. With appropriate understanding, these systems may be employed to build laser systems with ultra-short high intensity pulses. The traditional method of describing the phase delay introduced by these systems can be cumbersome at times. This thesis introduces a revised approach to calculating the phase delay in angularly dispersive systems. We also consider the energy flow in these systems. The group delay is usually derived by approximating the phase delay with the first few terms of a Taylor series expansion. We show that under a specific definition for the temporal position of a pulse, we can give a precise meaning to the group delay without approximation.

TABLE OF CONTENTS

LIST OF FIGURES

1. Introduction

Ultra-short high intensity lasers are an important tool in many modern fields of study. Their extremely short duration and high intensities allow researchers to pursue new experiments. In physics research, they are used to produce very hot plasmas and to probe high-field atomic physics. In our lab we are engaging in experiments to generate high-order harmonics, where a portion of the laser pulse in converted into coherent extreme ultraviolet radiation. Because the pulses can be made as short as a few femtoseconds, they give unprecedented temporal resolution for exploring fast chemical reactions and other fast phenomena.

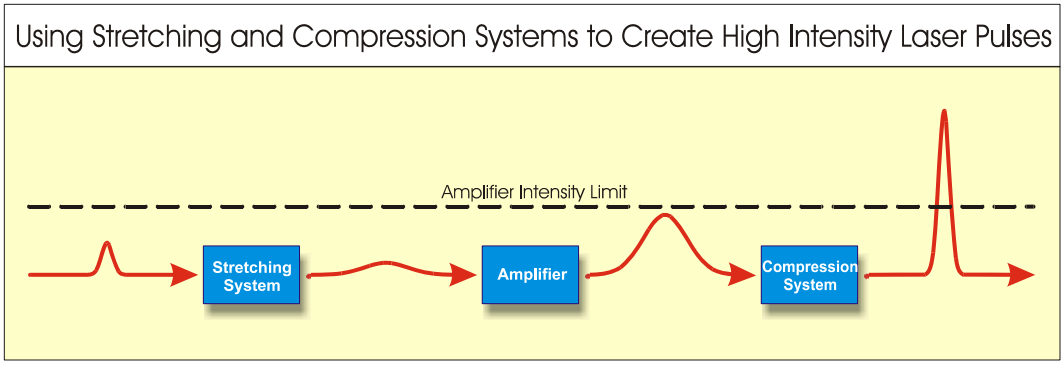

Figure 1 A schematic of the stretching-amplification-compression sequence used in chirp-pulse amplification. The limit placed on pulse intensities by the amplification material can be overcome by first stretching the laser pulse to a long temporal duration, amplifying this stretched pulse, and then re-compressing it. Using this technique, pulses with intensities of up to 10,000 times the amplifiers intensity limit can be generated.

There are several technical challenges in building short pulse lasers, especially when it is desired to achieve the highest possible intensity. One of the biggest challenges arises because high intensity light can damage the very materials used to amplify the light pulse. To overcome this limitation, laser physicists often employ a pulse stretching and compression technique, illustrated in Figure 1. This technique was first introduced by Mourou et al. in the late 1980's, and helps to keep the intensity from becoming too great while the pulse is being amplified. The first step is to low-intensity short pulses in an oscillator cavity. An individual pulse is then sent through a

stretching system, which spreads out the energy into a long temporal duration. In a typical stretching system, a pulse is stretched to thousands of times its original temporal duration. This relatively long pulse is then amplified to intensities permitted by the amplification material. The amplified pulse then passes through a system which compresses the pulse back to the original pulse duration, while retaining the energy gained in amplification. Because the energy is concentrated into a shorter pulse, the intensity of the light is proportionally increased. Using this technique, pulsed lasers produce intensities up to 10,000 times greater than can be achieved without the technique. The stretching and compression systems used in this process are examples of the angularly dispersive systems that are studied in this thesis.

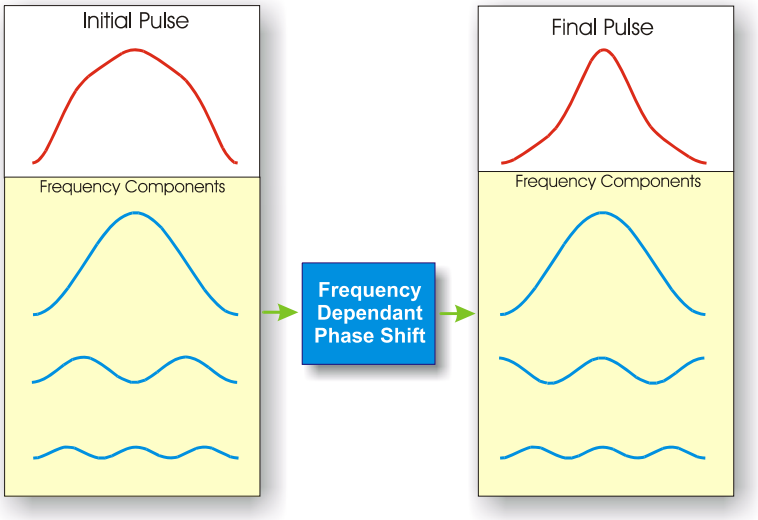

Figure 2 The superposition of three sine waves for two different phase configurations. The curves on top represent the summation of the three components beneath. The pulse on the left has the same frequency components as the one on the right. However, because the phase relations have been changed, the pulse on the right is narrower than the pulse on the left.

The pulse compression described above can be understood intuitively by examining the spectral composition of a pulse. We assume that a pulse can be represented as a summation of plane waves with different frequencies and intensities. The shape of the envelope of the pulse is determined by the spectral content of the pulse and the relative phases between the different

frequencies. By rearranging the phases of the different frequency components, we my greatly alter the temporal shape of the envelope while leaving the spectral content unchanged. To illustrate how this is done, consider a waveform illustrated in Figure 2 which is constructed by summing three frequency components. Imagine that we send this waveform through a system that introduces a frequency dependent phase shift – in this case the second frequency is shifted by π relative to the other frequencies. The resulting waveform is narrower than the original. Because we have restricted our spectrum to just three discrete frequencies in this example, the waveform is not a single pulse, but will repeat itself outside of the range shown. However, we may still use this phase rearranging technique to alter the shape of the pulse when the spectrum is expanded to include more frequencies, including the case of a continuous band of frequencies.

The goal for a laser pulse compression system is usually to rearrange the components in a manner that makes the envelope as narrow as possible in the temporal domain. One reason this is desirable is because of an inverse relationship between the duration and the intensity of the pulse. Thus, the shorter we make the pulse, the more intense it will be. The uncertainty relation $\Delta\omega\Delta t > 1$ places a limit on how narrow the pulse may be made, and hence on its intensity. When we are dealing with a pulse whose spectrum is characterized by a spread in frequencies given by $\Delta\omega$, we are fundamentally limited to pulse duration such that $\Delta t > 1/\Delta\omega$.

In this thesis, we will explore the analytic description of systems that introduce frequency dependent phase shifts using angular dispersion. These systems have been studied previously, and the traditional methods of analysis correctly describe the phase shift introduced by these systems. However, these descriptions are dependent on the specific geometry of each system, which can be cumbersome at times. We will show that the phase shift in these systems may be derived in a natural

and general way through a superposition of plane waves. The expression which results can be applied in a straight forward manner to a variety of systems even though the geometries differ. We also explore the traditional description of group delay which describes energy transport in the system. The conventional method for describing group delay involves an approximation using the first terms in a Taylor series expansion. In this context, group delay is a concept that begins to lose meaning if the shape of the pulse is significantly altered by dispersion. We will show that with a careful definition of the temporal position of a pulse, group delay has a precise meaning no matter how much the shape of the pulse is altered by dispersion.

2. Phase Shifts Associated with Angular Dispersion

There are many physical systems that can introduce frequency dependent phase shifts to the spectral components of a laser pulse. Many elements in short pulse laser systems employ the idea of angular dispersion to introduce the phase shifts. In an angularly dispersive system, different frequency components travel in different directions and therefore different distances. Some examples of systems that introduce phase shift in this manner are grating pairs, prism pairs, and material windows (illustrated in Figure 3). With appropriate understanding, these devices may be exploited to control the temporal characteristics of a laser pulse.

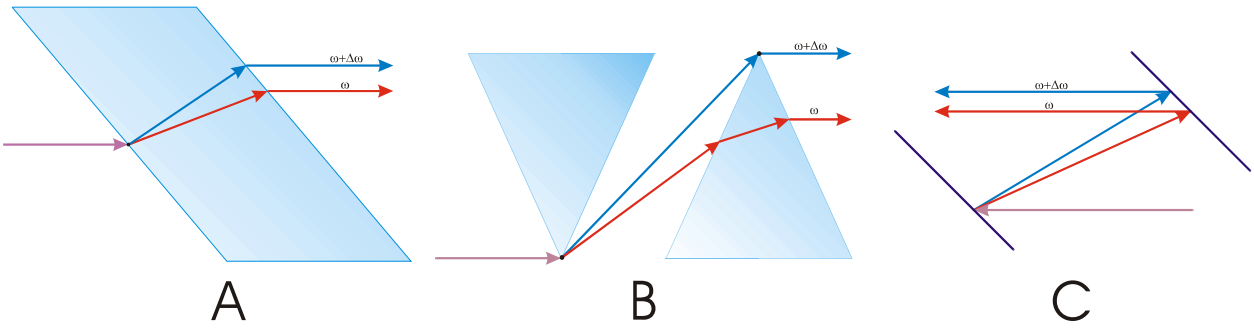

Figure 3 Angular dispersion represented (a) in a material window, (b) in a prism pair, and (c) in a parallel grating pair. Different frequencies travel different distances through the system because of their differing angles, and thus experience differing phase shifts. (a) represents a dielectric window with light incident at an angle. (b) represents an identical pair of prisms arranged so that the second prism "straightens out" the light refracted by the first prism. (c) shows a pair of identical diffraction gratings. Light is diffracted at the two gratings such that the outgoing pulse travels in the same direction as the incoming, but the different components travel different distances between the diffractions.

In order to see how these systems introduce phase shifts, consider two frequency components with frequencies ω and $\omega + \Delta\omega$ as they pass through the system. Examination of the figures shows that representative rays for the two frequencies will travel different distances through the systems. This difference will introduce the frequency dependent phase shift, $\phi(\omega)$, which is known as the *phase delay*. It is important to note that when calculating phase delay we must choose two points. We then say that the phase delay from one point to the other is given by $\phi(\omega)$.

Previous descriptions of these systems have been developed in terms of quasi ray pictures. In this method, the phase shift function is computed by examining the path of a representative ray for a given frequency as it traverses a system. To illustrate some of the complexities that are encountered using this method, we review the evaluation of $\phi(\omega)$ for a diffraction grating system using a representative ray approach. This system was analyzed by I. B. Treacy in a paper written in 1969.

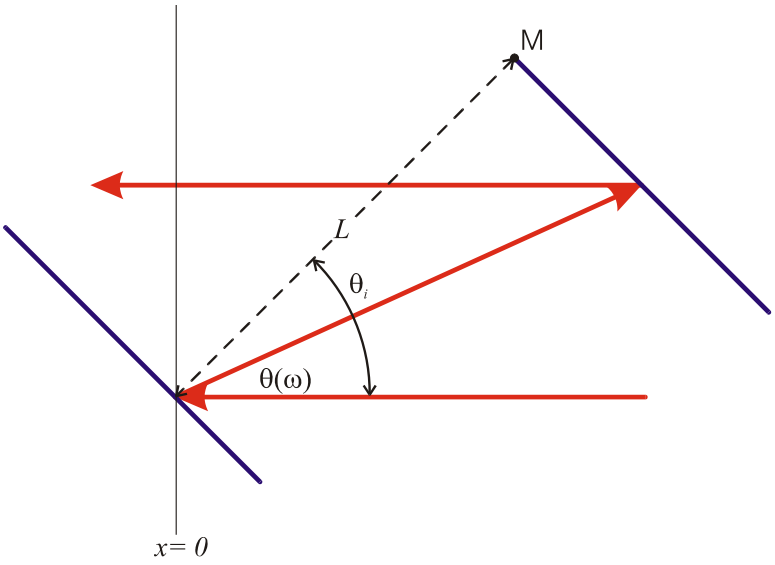

Figure 4 The geometry used to calculate phase delay for a diffraction grating system using traditional ray methods

The basic idea of the diffraction grating system is quite simple. A pulse incident on the first grating is diffracted according to the well known grating law $d\sin\left[\theta_i - \theta(\omega)\right] + d\sin\theta_i = \lambda$, where d is the spacing between grooves and λ is the wavelength for the frequency being considered. Assuming we are in vacuum, we can write $\lambda = 2\pi c/\omega$, and we can then write the angle $\theta(\omega)$ as

$$\theta(\omega) = \theta_i - \sin^{-1}\left[\frac{2\pi c}{\omega d} - \sin\theta_i\right]. \tag{1}$$

If the gratings are arranged parallel to one another then the incident angle for the second grating is the same as the reflected angle from the first, and so the angle of diffraction will also be the same. Thus we can readily see that the outgoing pulse travels in the same direction as the incoming, but the phase shift experienced in traversing the system is a function of frequency. In the region to the right of the system before the pulse first encounters a grating, the shape of the pulse profile remains constant as it moves to the left. This is also the case in the region to the left of the grating system after it encounters the second grating. In order to completely describe the system, we need to

calculate the phase delay accumulated in traveling from the plane $x = 0$ through the system (both grating hits) and back to $x = 0$. With an application of geometry and trigonometry, we can write the distance traveled by a representative ray in Figure 4 as

$$Path\ Length = \frac{L}{\cos\left[\theta(\omega)\right]} + \frac{L}{\cos\left[\theta(\omega)\right]}\cos\left[\theta_i - \theta(\omega)\right] = \frac{1+\cos\left[\theta_i - \theta(\omega)\right]}{\cos\left[\theta(\omega)\right]}. \quad (2)$$

The phase delay due to travel is then given by

$$\phi(\omega)_{travel} = \frac{\omega}{c}(Path\ Length) = \frac{\omega}{c}\frac{1+\cos\left(\theta_i - \theta(\omega)\right)}{\cos\left[\theta(\omega)\right]}. \quad (3)$$

To the point, the ray tracing approach seems quite straight forward. However, on closer inspection of the system we find that Eq. (2) does not completely describe the phase delay introduced in the system, however. To see why this is so, we examine Figure 5 which shows a plane wave front before and after refraction from the second diffraction grating. Because these are plane wave fronts, the phase at A and A' must be the same. Likewise the phase at C and C' must be equal. However, the paths ABC and A'B'C' are not equal, and this effect was not included when deriving Eq. (3). Treacy noted this discrepancy and gave the following explanation:

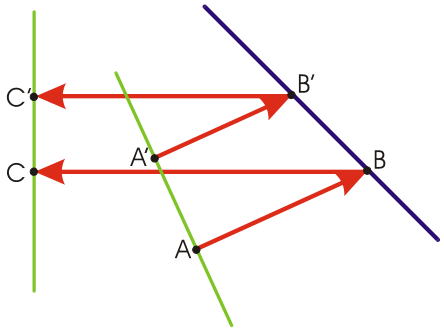

Figure 5 Depiction of a wave front diffraction from a grating. A'A and C'C represent wave fronts before and after refraction from the second grating. Because the paths ABC and A'B'C' are not equal we must add a phase matching term to the phase delay found in Eq. (3).

> The origin of this apparent discrepancy is in the nature of the phase matching between the two waves along the grating surface BB'. Grating diffraction may be characterized in terms of phase matching by a 2π phase jump at each ruling in first-order diffraction, 4π in second order, etc. For the first order diffraction considered here, one has to add 2π times the number of grating lines in the segment BB' to the phase shift along [A'B'C'] to make it equal the phase shift along [ABC]. (Treacy, 455)

To calculate this appended phase matching term, we must choose some reference point on the

second grating in order for the phase correction terms to be consistent. For simplicity, we choose point M in Figure 4. If the spacing between grooves is given by *d*, the number of grooves from point M to point B is given by

$$Number\ of\ Grooves = \frac{L}{d}\tan\left[\theta(\omega)\right]. \tag{4}$$

Finally, we are able to write down the total phase delay as

$$\phi(\omega) = \phi_{travel} - \phi_{matching} = \frac{\omega L}{c}\frac{1+\cos\left[\theta_i - \theta(\omega)\right]}{\cos\left[\theta(\omega)\right]} - 2\pi\frac{L}{d}\tan\left[\theta(\omega)\right]. \tag{5}$$

Eq. (5) correctly describes the phase delay for the diffraction grating system. However, the phase matching arguments used to find it are subtle and tend to obscure the source of the phase shift. In section 4 we present an alternative description of angularly dispersive systems. This new formulation includes the geometric details and phase matching features automatically into the description in a natural and straight forward way. It can also be easily applied to other systems such as the material window and prism pair.

3. Mathematical Background

In order to clarify the notation used in the rest of this thesis, we will now take a moment to review some of the basic mathematical concepts used. Assume that we have a knowledge of the electric field at some point $\vec{r}_0$ as a function of time, given by $\vec{E}(\vec{r}_0,t)$. The spectrum of this pulse at $\vec{r}_0$ is related to $\vec{E}(\vec{r}_0,t)$ through the Fourier Transform pair

$$\vec{E}(\vec{r}_0,\omega) = \frac{1}{\sqrt{2\pi}}\int_{-\infty}^{\infty}\vec{E}(\vec{r}_0,t)e^{i\omega t}dt \tag{6}$$

$$\vec{E}(\vec{r}_0,t) = \frac{1}{\sqrt{2\pi}}\int_{-\infty}^{\infty}\vec{E}(\vec{r}_0,\omega)e^{-i\omega t}d\omega \tag{7}$$

It is important to note that $\vec{E}(\vec{r}_0,\omega)$ is a complex vector, which contains the phase of the pulse. The

knowledge of $\vec{E}(\vec{r}_0,\omega)$ completely describes the field which passes point $\vec{r}_0$, but in order to describe the field at neighboring points we need to know the direction that each frequency component travels. The mathematical form for a plane wave of frequency ω is represented in the complex form by $e^{i(\vec{k}\cdot\vec{r}-\omega t)}$. The direction of wavevector $\vec{k}$ defines the direction of travel and must obey the dispersion relation $k(\omega) = n(\omega)\omega/c$, where $n(\omega)$ is the index of refraction for the medium in which the wave travels. If we assume a knowledge of $\vec{k}(\omega)$ at $\vec{r}_0$ we can write an expression for the electric field for all space and time as a superposition of plane waves (assuming no changes of medium or reflections). This is given by

$$\vec{E}(\vec{r},t) = \frac{1}{\sqrt{2\pi}}\int_{-\infty}^{\infty}\vec{E}(\vec{r}_0,\omega)e^{i(\vec{k}\cdot\Delta\vec{r}-\omega t)}d\omega \tag{8}$$

where $\Delta\vec{r} = \vec{r} - \vec{r}_0$ is the displacement from $\vec{r}_0$. Our analysis of angularly dispersive systems assumes, as does the traditional method, that there is only one wavevector associated with each frequency and that the medium in which we are propagating is uniform.

4. New Formulation

With the background provided in section 3, the derivation of the new method for finding $\phi(\omega)$ is quite straight forward. We begin the new description by assuming that we have a knowledge of the electric field at some point $\vec{r}_0$, given by the function $\vec{E}(\vec{r}_0,t)$. We might conveniently choose $\vec{r}_0$ to be a point on the first grating for a parallel grating pair, or at the first prism apex for a prism pair. $E(\vec{r}_0,\omega)$ is then described by Eq. (6). We also assume that we have a knowledge of $\vec{k}(\omega)$ at $\vec{r}_0$ so that $E(\vec{r},t)$ is specified by Eq. (7). As shown in Eq. (8), the field due to a frequency ω at a point displaced from $\vec{r}_0$ by $\Delta\vec{r}$ is

$$\vec{E}(\vec{r}_0 + \Delta\vec{r},\omega) = \vec{E}(\vec{r}_0,\omega)e^{i\vec{k}(\omega)\cdot\Delta\vec{r}}. \tag{9}$$

The point $\vec{r}_0 + \Delta\vec{r}$ might conveniently be chosen to be on the second grating in the case of a grating pair, or at the apex of the second prism for a prism pair. The contribution of each frequency to the net field at point $\vec{r}_0 + \Delta\vec{r}$ is related to the contribution at $\vec{r}_0$ through the phase term

$$\phi(\omega) \equiv \vec{k}(\omega) \cdot \Delta\vec{r} \,. \tag{10}$$

From this simple expression arises all of the detail contained in the more complicated ray approach used to derive Eq. (5). Eq. (10) is thus a general expression of the phase delay from $\vec{r}_0$ to $\vec{r}_0 + \Delta\vec{r}$. It requires only that we know the direction of travel as a function of frequency at some point, given by $\vec{k}(\omega)$. We can then calculate the phase delay at any other point in the medium.

To see how Eq. (10) make sense geometrically, consider Figure 6 which shows plane waves propagating in a medium. Because these are plane waves, the phase on any line segment parallel to a wave front is constant. Thus, we can evaluate the phase at any convenient point along a segment parallel to the wave front. The distance from $\vec{r}_0$ to D can be written as $l_k = \Delta r \cos\beta$

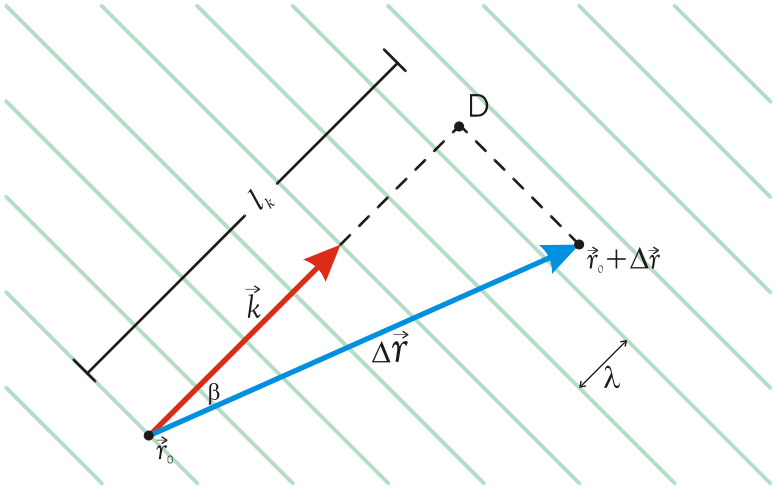

Figure 6 The geometry associated with Eq. (10).

where β is the angle between $\vec{k}$ and $\Delta\vec{r}$. As is evident from the figure, we can then write the phase as the optical path length multiplied by ω/c

$$\phi(\omega) = l_k n(\omega)\,\omega/c = \Delta r \cos(\beta) n(\omega)\,\omega/c\,, \tag{11}$$

which is equivalent to Eq. (10), and this shows the connection with the ray approach previously discussed.

Eq. (10) can be applied to a variety of spatially dispersive systems important for the control of the temporal profiles of short laser pulses. In grating pairs, prism pairs, and material windows, the angular spread of $k(\omega)$ is typically confined to a plane, say the x-y plane. In this case, we may write the phase term defined by Eq. (7) as

$$\phi(\omega) = \Delta x \frac{n(\omega)\omega}{c} \cos\left[\theta(\omega)\right] + \Delta y \frac{n(\omega)\omega}{c} \sin\left[\theta(\omega)\right], \tag{12}$$

where we have used the dispersion relation $k(\omega) = n(\omega)\omega/c$ and have explicitly entered the displacement of position in terms of its x and y components: $\Delta\vec{r} = \hat{\mathbf{i}}\Delta x + \hat{\mathbf{j}}\Delta y$. The angle $\theta(\omega)$ denotes the direction of the wavevector $k(\omega)$ with respect to the x-axis. Figure 7 illustrates the vectors, angles, and distances in connection with Eq. (12).

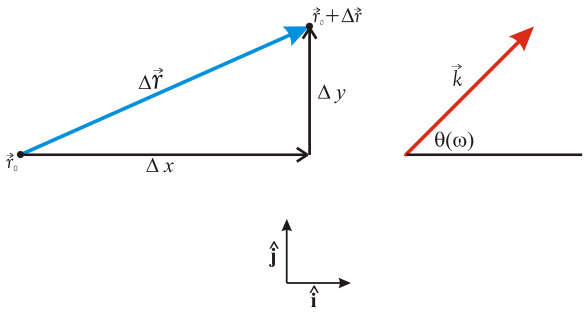

Figure 7 Positions associated with Eq. (12)

While writing the phase $\phi(\omega)$ in this form is not at variance with the traditional approach of using ray diagrams to assess phase delay, we will see in section 6 that the form in Eq. (12) will be particularly useful in assessing energy flow in such systems, wheras the ray method does not lend itself to this issue.

5. Sample Applications of the New Method

In this section we illustrate the utility of Eq. (12) by applying it to the three systems that we have been discussing. In these examples the geometric details and phase matching features are appropriately included automatically into the formulation. There will be no need to append phase matching arguments.

5.1 Grating Pair

We first return to the grating pair introduced in section 2. As noted in section 4, all we need to know in order to calculate the phase delay is the direction of travel as a function of frequency at some point. As before, the direction of travel is given by $\theta(\omega)$ in Eq. (1).

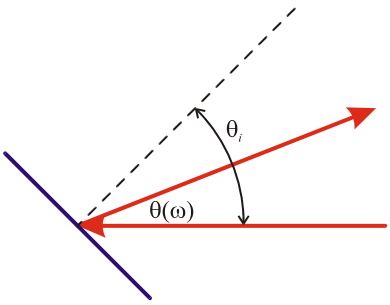

Figure 8 A depiction of the angle associated with each wavevector in a diffraction grating system.

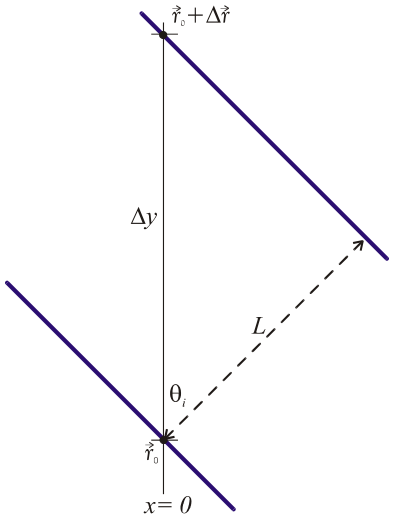

Figure 9 Convenient locations on a grating pair for evaluating phase delay through a system.

We next need to choose a point to evaluate the phase delay. The reference point $\vec{r}_0$ is chosen on the first grating and the final point is chosen directly above $\vec{r}_0$, as shown in Figure 9. $\Delta\vec{r}$ is then given

by

$$\Delta\vec{r} = \hat{\mathbf{j}}\frac{L}{\sin\theta_i}. \tag{13}$$

Now we can immediately write down the phase delay using Eq. (12):

$$\phi(\omega) = \frac{\omega L}{c}\frac{\sin\left[\theta(\omega)\right]}{\sin\theta_i} \tag{14}$$

At first glace, this expression seems to differ from the phase delay given in Eq. (5) which was found using the ray tracing and phase matching approach. With a some trigonometry, the two expressions can be shown to differ only by the constant $-2\pi L/d\tan\theta_i$. This constant gives us the number of grooves from $\vec{r}_0 + \Delta\vec{r}$ to point M in Figure 9 which we arbitrarily chose as our reference for phase matching. Since a constant phase shift does not affect pulse shape, the two approaches are equivalent for obtaining the form of the pulse.

5.2 Dielectric Window

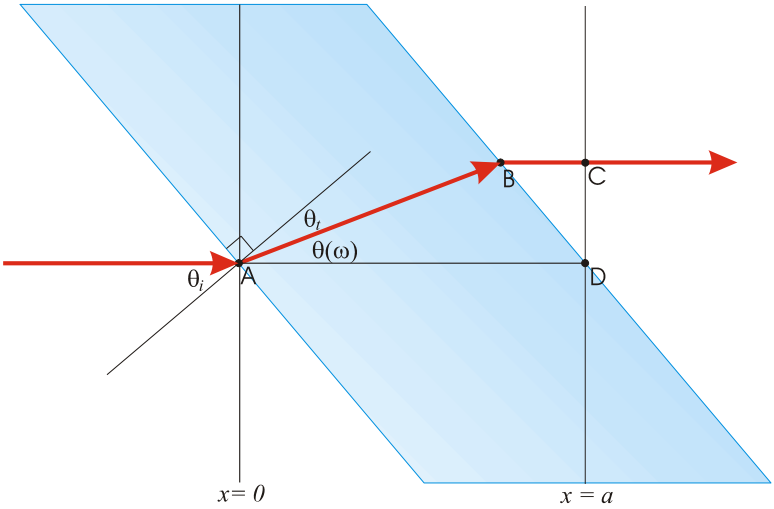

Figure 10 The geometry for calculating phase delay for a dielectric window with oblique incidence.

We next consider a system composed of a window of dielectric media which was mentioned in section 2. To use the traditional ray approach to calculate $\phi(\omega)$ from x=0 to x=a for this system

we must take into account the complexities that arise from the fact that the path ABC is not all in the same material. However, it is very straight forward to apply our alternative formulation. We choose $\bar{r}_0$ to be the point A on the window's first surface, as shown in Figure 10. $\theta(\omega)$ can be calculated using Snell's law as

$$\theta(\omega) = \theta_i - \sin^{-1}\left[\frac{\sin\theta_i}{n(\omega)}\right]. \tag{15}$$

Next we choose $\Delta\bar{r} = a\hat{\mathbf{i}}$ so that we are determining $\phi(\omega)$ at point D, we can immediately write down the phase delay without worrying about the geometric details required to analyze system using the ray approach. Applying Eq. (12) we immediately have

$$\phi(\omega) = a\frac{n(\omega)\omega}{c}\cos\left[\theta(\omega)\right], \tag{16}$$

which is in exact agreement the phase delay found using the ray tracing approach (Appendix A).

5.3 Prism Pair

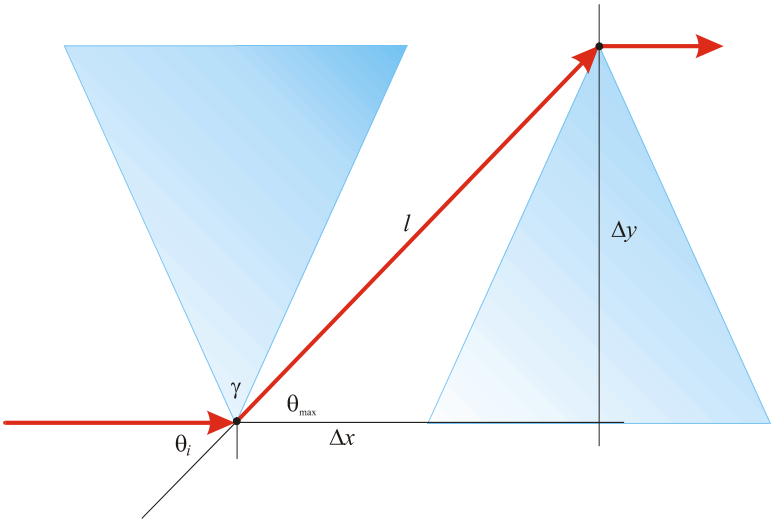

Figure 11 Geometry of a prism pair used to introduce dispersion

Finally we consider a prism pair system where two identical prisms arranged as shown in Figure 11. This system is used in laser systems when it is desired to adjust the duration of the pulse

by small amounts. In the new method of calculating phase, we determine the direction of travel as a function of frequency. With two applications of Snell's law, we can calculate the direction of travel as

$$\theta(\omega) = \theta_i - \alpha + \sin^{-1}\left[n(\omega)\sin\left(\alpha - \sin^{-1}\left[\frac{\sin\theta_i}{n(\omega)} \right] \right) \right]. \tag{17}$$

A convenient place to evaluate the phase delay is between the apices of the second prisms. Thus we can write the displacement as $\Delta\vec{r} = l_p \cos\theta_{\max}\hat{\mathbf{i}} + l_p \sin\theta_{\max}\hat{\mathbf{j}}$. After combining this result with Eq. (12) we can obtain

$$\begin{aligned} \phi(\omega) &= \frac{l_p n(\omega)\omega}{c}\left[\cos\theta_{\max}\cos\theta(\omega) + \sin\theta_{\max}\sin\theta(\omega) \right] \\ &= \frac{l_p n(\omega)\omega}{c}\cos\left[\theta_{\max} - \theta(\omega) \right] \end{aligned} \tag{18}$$

Again this result is in agreement with the ray tracing approach found in appendix A. In the case of a prism pair, the ray tracing method is rather tedious.

6. Energy Flow in Angularly Dispersive Systems

In the previous sections we have explored how passing through angularly dispersive systems changes the phase relations for the frequency components of a pulse. We now turn our attention to describing how energy flows inside the system itself. The Poynting vector averaged over individual field oscillations may be written as

$$\vec{S}(\vec{r},t) = \frac{1}{2}\vec{E}(\vec{r},t) \times \vec{H}^*(\vec{r},t) \ . \tag{19}$$

This average removes the rapid variations of the field associated with each cycle, resulting in a smooth time dependence which follows the temporal envelope of the field. When writing the Poynting vector in this way, we assume that the pulse envelope lasts at least several optical cycles so that oscillation averages are sensible. We can also consider the flow of energy in terms of

individual frequency components:

$$\vec{S}(\vec{r},\omega) = \frac{1}{2}\vec{E}(\vec{r},\omega) \times \vec{H}^{*}(\vec{r},\omega). \tag{20}$$

It is important to note that $\vec{S}(\vec{r},\omega)$ is not simply the Fourier transform of $\vec{S}(\vec{r},t)$. $\vec{S}(\vec{r},\omega)$ is defined by taking the Fourier transforms of $\vec{H}(\vec{r},t)$ and $\vec{E}(\vec{r}_0,t)$ separately and then performing the cross product multiplication. The electric field and magnetic intensity share a common phase. Thus, the phase delay derived in Eq. (10) and Eq. (12) for the electric field applies equally well to $\vec{H}(\vec{r},t)$.

The total energy per area is the same whether summed over time or over frequency. Mathematically, this is stated with Pareval's theorem:

$$\int_{-\infty}^{\infty} \vec{S}(\vec{r}_1,t)dt = \int_{-\infty}^{\infty} \vec{S}(\vec{r}_2,\omega)d\omega \ . \tag{21}$$

For this theorem to hold, the points $\vec{r}_1$ and $\vec{r}_2$ need not be the same within a uniform material.

An interesting aspect of pulse propagation within an angularly dispersive system is the time it takes for the energy of a pulse to traverse the system. Because of the dispersion, pulse shape and duration can evolve in complicated and perhaps asymmetric ways as it travels through a system. It therefore becomes necessary to define pulse arrival time in a way which does not carry an arbitrary dependence on the pulse shape. In this thesis, we define the temporal position of a pulse to be the average time of energy arrival.

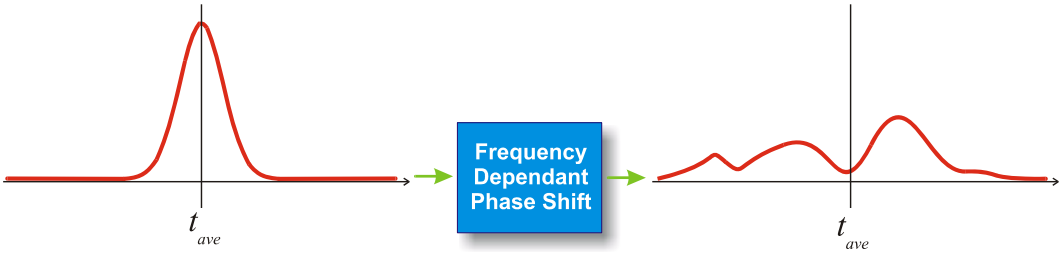

Figure 12 We define the temporal position of a pulse to be the average time of energy arrival. With this definition we can unambiguously discuss the temporal location of a pulse even after it has evolved in complicated ways because of dispersion. For the pulse on the left, it simple to visualize the pulse's temporal location. The pulse on the right shows schematically what the same pulse may look like after the shape is changed by dispersion. It is visually less obvious how to define the temporal position for this changed pulse, but the average time of energy arrival is still well defined.

This average time is found by weighting the time by the Poynting vector at position $\vec{r}_0$:

$$t_{ave}\left(\vec{r}_0\right) \equiv \hat{\mathbf{u}} \cdot \int_{-\infty}^{\infty} t\vec{S}\left(\vec{r}_0, t\right) dt \Big/ \hat{\mathbf{u}} \cdot \int_{-\infty}^{\infty} \vec{S}\left(\vec{r}_0, t\right) dt \,. \tag{22}$$

The arbitrary unit vector $\hat{\mathbf{u}}$ is introduced for convenience. It refers to the direction for which the energy flow is considered. It is an unimportant part of Eq. (22) since $\int_{-\infty}^{\infty} t\vec{S}\left(\vec{r}_0, t\right) dt$ and $\int_{-\infty}^{\infty} \vec{S}\left(\vec{r}_0, t\right) dt$ can be shown to be parallel. Using this definition, we show in Appendix C that the time from when a pulse passes position $\vec{r}_0$ until it arrives at $\vec{r}_1 = \vec{r}_0 + \Delta\vec{r}$ is given by

$$t_{ave}\left(\vec{r}_0 + \Delta\vec{r}\right) - t_{ave}\left(\vec{r}_0\right) = \hat{\mathbf{u}} \cdot \int_{-\infty}^{\infty} \vec{S}\left(\vec{r}_0, \omega\right) \frac{\partial \phi}{\partial \omega} d\omega \Big/ \hat{\mathbf{u}} \cdot \int_{-\infty}^{\infty} \vec{S}\left(\vec{r}_0, \omega\right) d\omega \,. \tag{23}$$

This formula shows precisely why $\partial\phi/\partial\omega$ is the group delay. The time delay between the energy arrival at the two positions is the sum of the group delays evaluated at individual frequencies weighted by their respective intensities. The energy of a pulse is delayed in accordance with the spectral content of the pulse regardless of how that energy is organized from one moment to the next. It is important to note that this formulation is exact rather than based on a Taylor's series expansion of the phase delay $\phi(\omega)$ centered about a specific frequency ω_0 as is traditionally done. In Eq. (23), the group delay $\partial\phi/\partial\omega$ is evaluated at every frequency present in the pulse.

The overall group delay for the pulse is the straight-forward linear superposition of the group delays evaluated at each of the individual frequencies present. While this conclusion might seem obvious in the end, it should be remembered that it is the field which obeys the primary linear superposition principle which gives rise to the interference pattern in space (according to the frequencies present with associated directions of travel and phases). The energy transport tracks quadratically the propagation of the interfering field amplitudes. The fact that this creates a new linear superposition principle for group delay may be viewed as remarkable.

7. Energy Transport

In Ref. [1] it was pointed out that for a parallel grating pair, the light associated with individual frequencies travels at speed c between bounces on the grating (assuming vacuum). An underlying theme of their approach was to circumvent cumbersome geometrical and phase matching analyses used by Treacy in the first examination of this system. Ref. [1] presents the argument that since variational methods can predict the path that an individual frequency of light travels through the system, the group delay at each frequency must be equal to the length of its path through the system divided by c. It should be noted, however, that variational methods are justified by the eikonal equation which is applicable for individual frequencies,[5] whereas the group delay $\partial\phi/\partial\omega$ by its nature involves neighboring frequencies. Therefore, an important link which is only implicit in Ref. [1] is that the net energy transport is the sum of the energy transported by the individual frequencies, as governed by the group delay evaluated at each frequency. This statement is expressed mathematically by Eq. (23) and is key to the conclusion.

For Eq. (23) to hold, it is not important that the frequency-dependent angular spread $\phi(\omega)$ of the light in the system be consistent with variational principles. In other words, the form of the angular function $\phi(\omega)$ is irrelevant to the conclusion. This assertion (to be discussed and supported below) is much broader than the premise of Ref. [1] where the central argument is that since variational methods specify $\phi(\omega)$, the energy transport of each frequency must occur along the specified angles at the speed of light. In other words, the conclusion that energy transport occurs along the path of each frequency at the speed of light is always true, even in situations where variational methods fail. For example, variational principles fail to produce the correct form of $\phi(\omega)$ in the case of an extraordinary ray when a birefringent material is used to make a prism pair

or a window. Nevertheless, the pulse delay is the sum of the individual group delays weighted by the spectrum according to Eq. (23).

The group delay at each frequency is found from the derivative of Eq. (12) which gives

$$\frac{d\phi}{d\omega} = \frac{1}{c}\left(n + \omega\frac{dn}{d\omega}\right)\left(\Delta x\cos\theta + \Delta y\sin\theta\right) + \frac{n\omega}{c}\frac{d\theta}{d\omega}\left(\Delta x\cos\theta - \Delta y\sin\theta\right). \tag{24}$$

If one considers the group delay along the specific direction that a particular frequency travels, then Eq. (24) simplifies and loses all dependence on $\theta(\omega)$, as was asserted above. A displacement along the direction described by $\theta(\omega)$ (the direction that frequency travels) is

$$\Delta\vec{r}_\omega \equiv \Delta r\left(\hat{\mathbf{i}}\cos\theta + \hat{\mathbf{j}}\sin\theta\right). \tag{25}$$

Substitution of this displacement into Eq. (25) yields

$$\left.\frac{d\phi}{d\omega}\right|_{\Delta\vec{r}_\omega} = \frac{\Delta r_\omega}{c}\left(n + \omega\frac{dn}{d\omega}\right), \tag{26}$$

which is the familiar group delay in a material which reduces to $\Delta r_\omega/c$ in the case of a grating pair in vacuum. The conclusion is that the group delay evaluated for any frequency is equal to the path for that frequency through the system divided the speed of light (group speed evaluated at that frequency). The functional form of $\theta(\omega)$ and whether it can be obtained by variational principles is irrelevant.

8. Conclusion

In summary, we have shown that systems that introduce a frequency dependent phase shift using angular dispersion can be described naturally considering the superposition of the individual waves. This description is generally applicable to many types of angularly dispersive systems. This new description avoids many of the geometric complexities and the phase matching arguments necessary in the traditional ray tracing approach. While both methods succeed in describing the

phase delay introduced by a system, the new method shows clearly how this phase delay comes naturally from the plane wave approximation of light.

Energy flow through angularly dispersive systems was also considered. We demonstrated that under a precise definition of energy arrival time, we can derive an exact form for the group delay. Using this new expression, we were able to show that the energy flow in these systems can be viewed as a linear superposition of its components.

REFERENCES

1. M. Born and E. Wolf, *Principles of Optics*, sixth edition, Pergamon press (New York 1980). Pp. 110-112.

2. C. H. Brito Cruz, P. C. Becker, R. L. Fork, and C. V. Shank, "Phase Correction of Femtosecond Optical Pulses Using a Combination of Prisms and Gratings," Opt. Lett. **13**, 123 (1988).

3. Brorson and Haus, "Diffraction Gratings and Geometric Optics," J Opt. Soc. Am. B **5**, 247 (1988).

4. C. G. Durfee III, S. Backus, M. M. Murnane, H. C. Kapteyn, "Design and Implementation of a TW-Class High-Average Power Laser System," IEEE J. of Quant. Electron. 4, 395 (1998).

5. Treacy, Edmond B. "Optical Pulse Compression with Diffraction Gratings," IEEE Journal of Quantum Electronics **QE-5**, 454 (1969).

APPENDIX A

PHASE DELAY FUNCTION FOR THE DIELECTRIC WINDOW AND PRISM PAIR (TRADITIONAL APPROACH)

To illustrate how the phase delay is calculated using a ray approach we consider dielectric windows and prism pairs in this appendix. In doing so, it the advantage of the revised approach becomes evident. First we consider the dielectric window with an optical pulse incident on the window at some arbitrary angle. The key to the ray tracing approach for computing $\phi(\omega)$ is to calculate the optical path length, l_p, for an arbitrary frequency. Then we can write the phase delay due to travel as

$$\phi(\omega) = l_p \frac{\omega}{c}. \tag{A.1}$$

Our task is then to find the optical path through the system for an arbitrary frequency. This is represented in Figure 14 by the path ABC. Consider the path for which the incident plane wave is not refracted at all ($n(\omega) = 1$), shown in figure 13 by the path AD. Any frequency for which $n(\omega) > 1$ will be refracted such that it $\vec{k}(\omega)$ will make an angle $\theta(\omega)$ with AD. Using Snell's law, we write

$$\theta(\omega) = \theta_i - \sin^{-1}\left[\frac{\sin\theta_i}{n(\omega)}\right]. \tag{A.2}$$

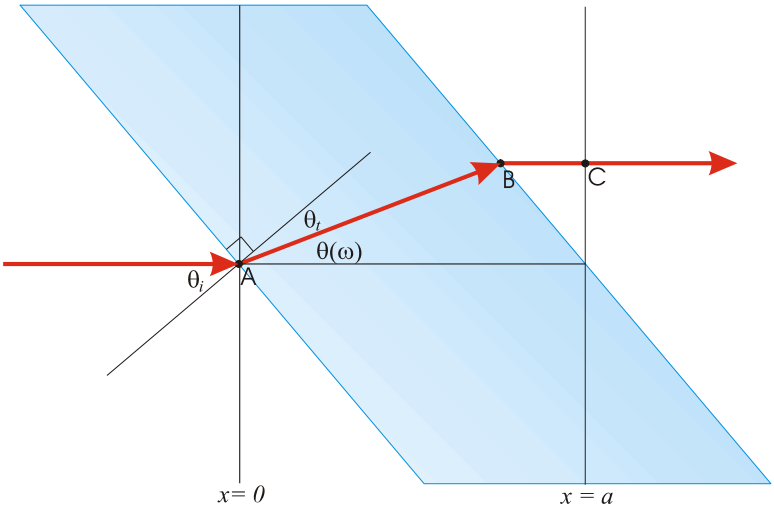

Figure 14 The geometry associated with finding the phase delay for a dielectric window using the ray tracing method.

Because the path AB is inside the material while BC is outside of the material we must write our optical path in two pieces. Using geometry and trigonometry these can be obtained as

$$l_{AB} = n(\omega)\frac{a\cos\left[\theta_t + \theta(\omega)\right]}{\cos\theta_t} \tag{A.3}$$

$$l_{BC} = a - \frac{a\cos\left[\theta(\omega)\right]\cos\left[\theta_t + \theta(\omega)\right]}{\cos\theta_t} \tag{A.4}$$

Combining these two expression with Eq. (A.1) we can then write the phase delay as

$$\phi(\omega) = \frac{\omega}{c}\left[n(\omega)\frac{a\cos\left[\theta_t + \theta(\omega)\right]}{\cos\theta_t} + a - \frac{a\cos\left[\theta(\omega)\right]\cos\left[\theta_t + \theta(\omega)\right]}{\cos\theta_t}\right] \tag{A.5}$$

The prism pair is a little more geometrically complex.

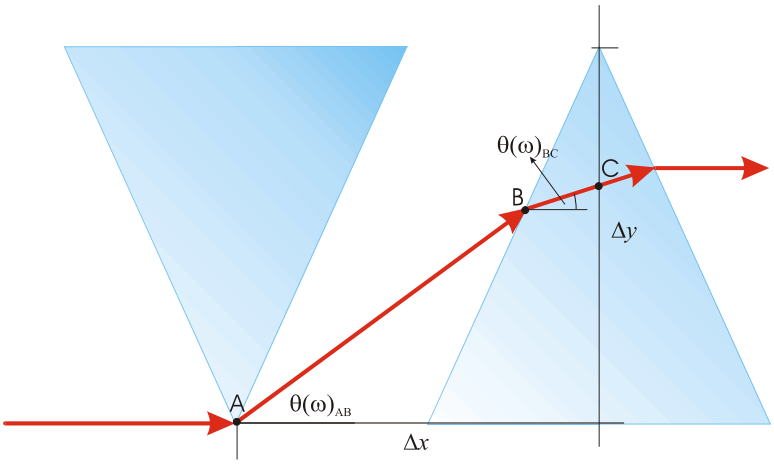

Figure 15 The geometry associated with the ray tracing method for finding phase delay in the case of a prism pair.

The angle associated with the path from A to B is again given by

$$\theta(\omega)_{AB} = \theta_i - \alpha + \sin^{-1}\left[n(\omega)\sin\left(\alpha - \sin^{-1}\left[\frac{\sin\theta_i}{n(\omega)} \right] \right) \right] \tag{A.6}$$

The angle associated with the path from B to C can be written using Snell's law and some geometry as

$$\theta(\omega)_{BC} = \sin^{-1}\left[\frac{\sin\left[\theta(\omega)_{AB} - \alpha/2\right]}{n(\omega)} \right] - \frac{\alpha}{2} \tag{A.7}$$

We can then write the two optical paths as

$$l_{AB} = \frac{\Delta x \cot(\alpha/2) - \Delta y}{\sin\left[\theta(\omega)_{AB}\right] - \cos\left[\theta(\omega)_{AB}\right]\cot(\alpha/2)} \tag{A.8}$$

$$l_{BC} = \frac{n(\omega)}{\cos\left[\theta(\omega)_{BC}\right]}\left[\Delta x - \frac{\Delta x \cot(\alpha/2) - \Delta y}{\tan\left[\theta(\omega)_{AB}\right] - \cot(\alpha/2)}\right] \tag{A.9}$$

And we can write the total phase delay as

$$\phi(\omega) = \frac{\omega}{c}\left(l_{AB} + l_{BC}\right) \tag{A.10}$$

APPENDIX B

CODE USED TO GENERATE THE POYNTING VECTOR PLOT

The following Delphi code plots Eq. (20) for the case of a diffraction grating. It was used to generate the images for Figure 14.

```
procedure TfrmMain.GeneratePlot(Sender: TObject);
Const
  step = 8;
  imax = ArraySize Div 2;
  jmax = imax Div step;
  kmax = imax Div step;
  gamma = 20*3.14159/180;
  d  = 1.0;
  c  = 0.3;
  dt = 2.667/100;
  dw = 6.28318/(dt*Imax);
  w0 = 6.28318*c/0.8;
  tau= 200.0*dt;
  Emax = 1.0;
Var
    I, J, K ,I2: Integer;
    E, Ex, Ey, Hz : gldArray;
    Sx, Sy, p : Real;
    theta, w, t, x, y, dx : Real;
    arg, cgt, sgt, ca, sa, scgct : Real;
    Bitmap : TBitmap;
    DataFile:TextFile;
begin
  Bitmap := TBitmap.Create;
  Bitmap.Width := 512;
  Bitmap.Height := 512;

  For I := 1 to Imax do Begin
    t := dt*(I-1-Imax/2);
    E[2*I-1] := Emax * exp(-(t/tau)*(t/tau));
    E[2*I] := 0.0;
  End;

{  AssignFile(DataFile,'Data1.txt');
  Rewrite(DataFile);
  For I := 1 to (ArraySize Div 2) do Begin
```

```
    Writeln(DataFile,E[I*2-1]:0:3,#9,E[I*2]:0:3);
  End;
  CloseFile(DataFile);}

  Spectrum(E,dw,Imax);
  AssignFile(DataFile,'Data.txt');
  Rewrite(DataFile);

  dx := c*dt*step*cos(gamma);
  For J := 1 to Jmax do Begin
    Gauge.Progress := Trunc(J/Jmax*100);
    x := dx*(J-Jmax/2);
    y := x*tan(gamma);
    theta := 0.0;
    For I := 1 to Imax do Begin
      w := dw*(I-1-Imax/2);
      arg := 6.28318*c/((w+w0)*d)-sin(gamma);
      If abs(arg) <= 1 then theta := arcsin(arg);
      cgt := cos(gamma-theta);
      sgt := sin(gamma-theta);
      arg := (w+w0)/c*(cgt*x+sgt*y);
      ca := cos(arg);
      sa := sin(arg);
      scgct := sqrt(cos(gamma)/cos(theta));
      I2 := 2*I;
      Ex[I2-1] := (E[I2-1]*ca-E[I2]*sa) * (-sgt)*scgct;
      Ex[I2]   := (E[I2-1]*sa+E[I2]*ca) * (-sgt)*scgct;
      Ey[I2-1] := (E[I2-1]*ca-E[I2]*sa) * cgt*scgct;
      Ey[I2]   := (E[I2-1]*sa+E[I2]*ca) * cgt*scgct;
      Hz[I2-1] := (E[I2-1]*ca-E[I2]*sa) * scgct;
      Hz[I2]   := (E[I2-1]*sa+E[I2]*ca) * scgct;
    End;
    Field(Ey,dt,imax);
    Field(Ex,dt,imax);
    Field(Hz,dt,imax);

    For K := 1 to Kmax do Begin
      I := K*Step;
      I2 := 2*I;
      Sx := Ey[I2-1]*Hz[I2-1]+Ey[I2]*Hz[I2];
      Sy := -Ex[I2-1]*Hz[I2-1]-Ex[I2]*Hz[I2];
      P := sqrt(Sx*Sx+Sy*Sy);
      If x=0 then P := 1.;
      Write(DataFile,P:0:3,#9);
      Bitmap.Canvas.Pixels[J-1,K-1] := getColor(P);
    End;
    WriteLn(DataFile);
  End;
  Graph.Picture.Bitmap.Assign(Bitmap);
  Graph.Picture.Bitmap.SaveToFile('Plot1.bmp');
  CloseFile(DataFile);

end;
```

APPENDIX C

DERIVATION OF PHASE DELAY BETWEEN TWO POINTS

In this appendix we seek an expression for the time it takes for a pulse to travel from $\vec{r}_0$ to a point $\vec{r}_1$ separated from $\vec{r}_0$ by Δr. The time of arrival at $\vec{r}_0$ is given by Eq. (22), and we may write a corresponding expression for the time of arrival at $\vec{r}_1$:

$$t_{ave}\left(\vec{r}_1\right) = \hat{\mathbf{u}} \cdot \int_{-\infty}^{\infty} t\vec{E}\left(\vec{r}_1, t\right) \times \vec{H}^*\left(\vec{r}_1, t\right) dt \Big/ \hat{\mathbf{u}} \cdot \int_{-\infty}^{\infty} \vec{S}\left(\vec{r}_1, \omega\right) d\omega \tag{C.1}$$

Because we are dealing with plane waves and assume that energy is conserved, the Poynting vector integral in the denominator must be the same whether we consider $\vec{r}_1$ or $\vec{r}_0$. Thus we have

$$t_{ave}\left(\vec{r}_1\right) = \hat{\mathbf{u}} \cdot \int_{-\infty}^{\infty} t dt \tfrac{1}{\sqrt{2\pi}} \int_{-\infty}^{\infty} \vec{E}\left(\vec{r}_1, \omega\right) e^{-i\omega t} d\omega \times \tfrac{1}{\sqrt{2\pi}} \int_{-\infty}^{\infty} \vec{H}^*\left(\vec{r}_1, \omega'\right) e^{-i\omega' t} d\omega' \Big/ \hat{\mathbf{u}} \cdot \int_{-\infty}^{\infty} \vec{S}\left(\vec{r}_0, \omega\right) d\omega \ , \tag{C.2}$$

where we have also replaced $\vec{E}\left(\vec{r}_1, t\right)$ and $H^*\left(\vec{r}_0, t\right)$ with their Fourier transform representation. We then rearrange the order of integration so that we have

$$t_{ave}\left(\vec{r}_0\right) = \hat{\mathbf{u}} \cdot \int_{-\infty}^{\infty} \vec{E}\left(\vec{r}_1, \omega\right) d\omega \times \int_{-\infty}^{\infty} \vec{H}\left(\vec{r}_1, \omega'\right) d\omega' \frac{1}{2\pi} \int_{-\infty}^{\infty} t e^{-i(\omega - \omega')t} dt \Big/ \hat{\mathbf{u}} \cdot \int_{-\infty}^{\infty} \vec{S}\left(\vec{r}_0, \omega\right) d\omega \ . \tag{C.3}$$

For reasons that will become clear later, we rewrite the last to terms of the numerator as a partial derivative with respect to ω. Then we may write

$$t_{ave}(\vec{r}_1) = \hat{\mathbf{u}} \cdot \int_{-\infty}^{\infty} \vec{E}(\vec{r}_1, \omega) d\omega \times \frac{\partial}{\partial \omega} \int_{-\infty}^{\infty} \vec{H}^*(\vec{r}_1, \omega') d\omega' \frac{i}{2\pi} \int_{-\infty}^{\infty} e^{-i(\omega-\omega')t} dt \Big/ \hat{\mathbf{u}} \cdot \int_{-\infty}^{\infty} \vec{S}(\vec{r}_0, \omega) d\omega \qquad \text{(C.4)}$$

Next, we note that the last term of the numerator is a representation of the delta function and we have

$$t_{ave}(\vec{r}_1) = i\hat{\mathbf{u}} \cdot \int_{-\infty}^{\infty} \vec{E}(\vec{r}_1, \omega) d\omega \times \frac{\partial}{\partial \omega} \int_{-\infty}^{\infty} \vec{H}^*(\vec{r}_1, \omega') \delta(\omega - \omega') d\omega' \Big/ \hat{\mathbf{u}} \cdot \int_{-\infty}^{\infty} \vec{S}(\vec{r}_0, \omega) d\omega \qquad \text{(C.5)}$$

The second integration in the numerator is then easily carried out to leave

$$t_{ave}(\vec{r}_1) = i\hat{\mathbf{u}} \cdot \int_{-\infty}^{\infty} \vec{E}(\vec{r}_1, \omega) \times \frac{\partial}{\partial \omega} \vec{H}^*(\vec{r}_1, \omega) d\omega \Big/ \hat{\mathbf{u}} \cdot \int_{-\infty}^{\infty} \vec{S}(\vec{r}_0, \omega) d\omega \qquad \text{(C.6)}$$

Our next step is to evaluate the partial derivative in the numerator. First note that by definition we have that $\vec{E}(\vec{r}_1, \omega) = \vec{E}(\vec{r}_0, \omega) e^{-i\phi(\omega)}$, where $\phi(\omega)$ is the phase delay in moving from $\vec{r}_0$ to $\vec{r}_1$. Using the chain rule we can carry out the derivative:

$$\frac{\partial}{\partial \omega} H(\vec{r}_1, \omega) = \frac{\partial}{\partial \omega} \left[e^{-i\phi(\omega)} H(\vec{r}_0, \omega) \right]$$

$$= e^{-i\phi(\omega)} \frac{\partial}{\partial \omega} H(\vec{r}_0, \omega) - ie^{-i\phi(\omega)} H(\vec{r}_0, \omega) \frac{\partial}{\partial \omega} \phi(\omega) \qquad \text{(C.7)}$$

We substitute the derivative back into Eq. (B.6) to obtain

$$t_{ave}(\vec{r}_1) = i\hat{\mathbf{u}} \cdot \int_{-\infty}^{\infty} \vec{E}(\vec{r}_1,\omega) e^{-i\phi(\omega)} \times \left(\frac{\partial}{\partial\omega} H^*(\vec{r}_0,\omega) - iH^*(\vec{r}_0,\omega) \frac{\partial}{\partial\omega}\phi(\omega) \right) \Big/ \hat{\mathbf{u}} \cdot \int_{-\infty}^{\infty} \vec{S}(\vec{r}_0,\omega) d\omega , \tag{C.8}$$

and rearrange the terms to find

$$t_{ave}(\vec{r}_1) = \left(i\hat{\mathbf{u}} \cdot \int_{-\infty}^{\infty} \vec{E}(\vec{r}_0,\omega) \times \frac{\partial}{\partial\omega} \vec{H}^*(\vec{r}_0,\omega) d\omega + \hat{\mathbf{u}} \cdot \int_{-\infty}^{\infty} \frac{\partial\phi(\omega)}{\partial\omega} \vec{S}(\vec{r}_0,\omega) d\omega \right) \Big/ \hat{\mathbf{u}} \cdot \int_{-\infty}^{\infty} \vec{S}(\vec{r}_0,\omega) d\omega . \tag{C.9}$$

If we imagine for a moment that we chose points such that $\vec{r}_0 = \vec{r}_1$, then by definition $\phi(\omega) = 0$. We are left with

$$t_{ave}(\vec{r}_0) = i\hat{\mathbf{u}} \cdot \int_{-\infty}^{\infty} \vec{E}(\vec{r}_0,\omega) \times \frac{\partial}{\partial\omega} \vec{H}^*(\vec{r}_0,\omega) d\omega \Big/ \hat{\mathbf{u}} \cdot \int_{-\infty}^{\infty} \vec{S}(\vec{r}_0,\omega) d\omega . \tag{C.10}$$

Finally, we substitute Eq. (40) into Eq. (39) for our complete expression

$$t_{ave}(\vec{r}_0 + \Delta\vec{r}) - t_{ave}(\vec{r}_0) = \hat{\mathbf{u}} \cdot \int_{-\infty}^{\infty} \vec{S}(\vec{r}_0,\omega) \frac{\partial\phi}{\partial\omega} d\omega \Big/ \hat{\mathbf{u}} \cdot \int_{-\infty}^{\infty} \vec{S}(\vec{r}_0,\omega) d\omega \tag{C.11}$$

which is discussed in section 6.